Draft version February 13, 2015
Preprint typeset using LaTeX style emulateapj v. 08/13/06

MONTE CARLO METHOD FOR CALCULATING UNCERTAINTY IN OXYGEN ABUNDANCE FROM STRONG-LINE FLUX MEASUREMENTS

Author order to be determined: Maryam Modjaz[1], Federica Bianco[1], Seung Man Oh[1,2], David Fierroz[1], Yuqian Liu[1], Lisa Kewley[3,4]

Draft version February 13, 2015

ABSTRACT

MODIFY & FINALIZE AT THE END: We present an open-source Python code for the determination of the strong-emission-line estimators of oxygen abundance in the standard scales, based on the original IDL-code in Kewley & Dopita (2002). The standard strong line Metallicity scales and diagnostics IMPROVE have been used to estimate metal abundance by using emission line ratios. Here we introduce Monte Carlo resampling to these methods in order to better characterize an oxygen abundance confidence region. We output probability distributions, measured values for metallicity and, when desired, for reddening E(B-V). We test our code on emission lines measurements from a sample of galaxies ($z < 0.15$) and compare our metallicity results with those from previous methods. . We show that our metallicity estimate is consistent with previous methods but yields smaller uncertainties. The code is open source and can be found at www.github.com/snyugroup.

Subject headings:

1. INTRODUCTION

The low quantity of carbon, oxygen, nitrogen, sulfur and iron among other elements provide a splash of color to the otherwise dominating greyscape of hydrogen and helium in the stars and gas of galaxies. Nevertheless, even the minute presence of heavy elements (all elements heavier than H and He, also called metals or collectively metallicity) is important for many areas of astrophysics. For example, Johnson & Li (2012) suggest that if it was not for the relatively high metallicity level in our solar system, planet formation may not have been possible. With Z representing the mass fraction of metals, for own sun the value is measured to be Z=0.0153 (Caffau et al. 2011), though there are others who suggest a lower solar metallicity of Z=0.0134 in particular because of oxygen (Asplund et al. 2009; Grevesse et al. 2010)[5]. Furthermore, when properly observed and estimated, metallicity measurements of the galactic gas can tightly constrain models of galaxy formation and evolution (e.g., Kewley & Ellison 2008 and references therein), as well as shed light on the metallicity dependence and production conditions for different types of SNe and long-duration GRBs (e.g., Modjaz et al. 2008; Levesque et al. 2010; Anderson et al. 2010; Modjaz et al. 2011; Kelly & Kirshner 2012; Sanders et al. 2012).

However, for almost all astronomical objects, metallicity cannot be measured directly. The oxygen abundance in the gas-phase is the canonical choice of metallicity indicator for interstellar medium (ISM) studies, since oxygen is the most abundant metal and only weakly depleted onto dust grains (in contrast to refractory elements such as Mg, Si, Fe, with Fe being depleted by more than a factor of 10 in Orion; see Simón-Díaz & Stasińska 2011). The oxygen abundance[6] is expressed as $12 + \log_{10}(\frac{O}{H})$ where O and H are the number fractions of Oxygen and Hydrogen, respectively. Importantly, oxygen exhibits very strong nebular lines in the optical wavelength range of HII regions (e.g., Pagel et al. 1979; Osterbrock 1989; Tremonti et al. 2004), and thus, many different diagnostic techniques have been developed (e.g., Kewley & Dopita 2002; Pettini & Pagel 2004; Kobulnicky & Kewley 2004; Kewley & Ellison 2008), which are discussed in the next section.

1.1. *The different oxygen abundance diagnostics*

The "classical" way to estimate the oxygen abundance is the electron temperature (T_e) method, which estimates the electron temperature and density of the nebula using a number of oxygen lines with different ionization states, including the auroral [OIII] λ4363 line, to then directly estimate the OII and OIII abundances to obtain the total oxygen abundance, after correcting for the unseen stages of ionization. However, the auroral [OIII] λ4363 line is very weak, even in low-metallicity environments, and saturates at higher metallicity (since oxygen NIR fine structure lines are cooling the nebula at higher metallicities) − thus, other methods had to be developed that use other, stronger lines, in the spectra of HII regions. **MENTION DOPITA's results since the SN people are not aware of the recent developements** These are called strong-line methods and are the subject of this manuscript. Strong-line methods can be basically categorized into two types: theoretical methods, that rely on calibrating various observed line ratios using photoionization methods (basically theoretically simulating HII regions, using stellar model atmospheres, stellar

[1] Center for Cosmology and Particle Physics, New York University, 4 Washington Place, New York, NY 10003, USA
[2] NYU Abu Dhabi PO Box 129188 Abu Dhabi, UAE
[3] Australian National University, Research School for Astronomy & Astrophysics, Mount Stromlo Observatory, Cotter Road, Weston, ACT 2611, Australia
[4] Institute of Astronomy, University of Hawaii, 2680 Woodlawn Drive, Honolulu, HI 96822, USA

[5] Note that these abundances refer to the current abundances in the sun, which are lower than the value with which the sun was formed 4.56 Gyr ago, since diffusion at the bottom of the convection zone has decreased metallicity over time (Grevesse et al. 2010).

[6] We note that in many cases in the literature, including here, the terms metallicity and oxygen abundance are used interchangeably.

populations and photoionization models) and empirical ones that calibrate various observed line ratios using observed T_e-based metallicities.

For the theoretical strong-line method, one ratio that is commonly used to determine the metallicity of galaxies is ([OII] λ3727 + [OIII] $\lambda 4959, \lambda 5007$)/$H_\beta$ (Pagel et al. 1979) and is referred to as R23. The drawback of this method is that it is double-valued with metallicity, and thus other line ratios need to be used to break the degeneracy between the high values ("upper branch") and the low values ("lower branch") of the R23 metallicities. Furthermore, Kewley & Dopita (2002) showed the importance of ionization parameter, which can be physically understood to correspond to the maximum velocity of an ionized front that can be driven by the local radiation field of hot massive stars that are ionizing the ISM gas. This ionization parameter needs to be taken into account in the various strong-line methods, as HII regions at the same metallicity but with different ionization parameters produce different line strengths. Calibrations of R23 by McGaugh (1991) (hereafter M91) and by Kewley & Dopita (2002) (hereafter KD02) use different theoretical photoionization models and take ionization parameter into account, while other calibrations such as of Zaritsky et al. (1994) (hereafter Z94) do not. Thus, Z94 is mostly valid for only metal-rich galaxies. M91 and KD02 use an iterative process to break the R23 degeneracy (KD02 uses different ratios [NII]/[OII] and [NII]/H_α) and to also constrain the ionization parameter q in order to arrive at the metallicity estimate.

As to empirical strong-line methods, the most commonly used one is that by Pettini & Pagel (2004) (hereafter PP04). PP04 used HII regions with Te-based metallicities to derive empirical fits to strong-line ratios, and introduce the line ratios of ([NII]/H_α (N2) and ([OIII]/H_β)/([NII]/H_α (O2N2) as metallicity diagnostics. Since PP04-N2 employs two closely spaced lines (Halpha and NII), which are not affected by stellar absorption, nor uncertain reddening, and are easily observed in one simple spectroscopic setup, it has become an often-used scale for at least low-z SN host galaxy studies (e.g. see metal-analysis by e.g,. Sanders et al. (2012); Modjaz (2012); Leloudas et al. (2014). However, it is important to remember that this scale has a number of short-comings: it does not take into account the impact of ionization parameter, was initially derived based on only 137 extragalactic HII regions, and the nitrogen emission line employed saturates at high metallicity (CHECK!), and thus this method may not be well-suited for high-metallicity galaxies. An updated calibration by Marino et al. (2013) based on many more Te-based metallicities (almost three time larger that that of PP04) derives a significantly shallower slope between O3N2 index and oxygen abundance than the PP04 calibration.

As can be seen, each scale has different advantages and disadvantages and may be used in different metallicity regimes (see detailed discussion in e.g., Kewley & Dopita 2002; Stasińska 2002; Kewley & Ellison 2008; Moustakas et al. 2010; Dopita et al. 2013; Blanc et al. 2015). Thus, this open-source code outputs the oxygen abundance in the main 6 metallicity scales (for which the KD02 diagnostic has four outputs and the PP04 diagnostic has two outputs). While there is a long-standing debate about which diagnostic to use, as there are systematic metallicity offsets between different methods (recombination lines vs. strong-line method vs. "direct" T_e method, see the above sources), *the relative metallicity trends can be considered robust, if the analysis is performed self-consistently in the same scale, and trends are seen across different scales (Kewley & Ellison 2008; Moustakas et al. 2010).* Note however, that while there are conversion values between different scales (Kewley & Ellison 2008), they apply for large data sets, since those conversion values were derived based on ten thousands of SDSS galaxies, and thus should be used with caution (or not at all) for smaller samples. In addition, there the debate about the value of the solar oxygen abundance value (Asplund et al. 2009; Caffau et al. 2011), such that the absolute oxygen calibration is still uncertain.

Here we introduce the open-source code "". pro .. In § 2 we describe our method, the input and output values of the code. In § 4, we compare our method of obtaining abundance uncertainties to previous methods in the literature.

2. DESCRIPTION OF METALLICITY CODE

For computing oxygen abundances, we use the iterative code by Kewley & Dopita (2002), which has been updated in Kewley & Ellison (2008) and reflects .. **LISA: YOUR INPUT HERE:what is the update??** which was initially written in IDL. We translated it into python, added the new feature of obtaining uncertainties on the metallicity outputs via Monte Carlo resampling, and made it open source via github, as we explain below.

We assume that the observed emission lines to be used to indicate metallicity originate in HII regions and are not due to non-thermal excitation by e.g., AGN or interstellar shocks from SNe or stellar winds. Tests to exclude data contaminated by such non-thermal sources have to be executed by using the recommended line ratios by e.g., Baldwin et al. 1981; Kauffmann et al. 2003; Kewley et al. 2006 prior to running this code. Furthermore these lines should have all the correct calibration (at least correct relative calibration) and should have a signal-to-noise ratio (S/N) of at least 3. The latter is important for the success of the Monte Carlo resampling technique as described below.

2.1. *Input and Output of code*

Emission line flux values are fed into our Python implementation as in the original code by Kewley & Dopita, which is written in IDL and hereafter referred to as IDL02. The inputs are emission line flux values and their uncertainties for the following lines: Hα, Hβ, [OI] 6300, [OII] 3727, [OIII] 4959, [OIII] 5007, [NII] 6584, [SII] 6717, [SII] 6731, SIII 9532, and SIII 9096 **CHECK!** and their uncertainties. If the fluxes for the specified lines are not available, the entry is left to 0 and the outputted oxygen abundance scales will be in only metallicity scales that use the line fluxes provided. As part of the code, the inputted line fluxes are corrected for reddening by using the observed Balmer decrement, for which Hα and Hβ flux values are needed to be provided. We assume case B recombination and thus, the standard value of 2.86 as the intrinsic Hα/Hβ ratio (Osterbrock 1989), and apply the standard Galactic reddening law with R_V = 3.1 (Cardelli et al. 1989). However, the user can choose

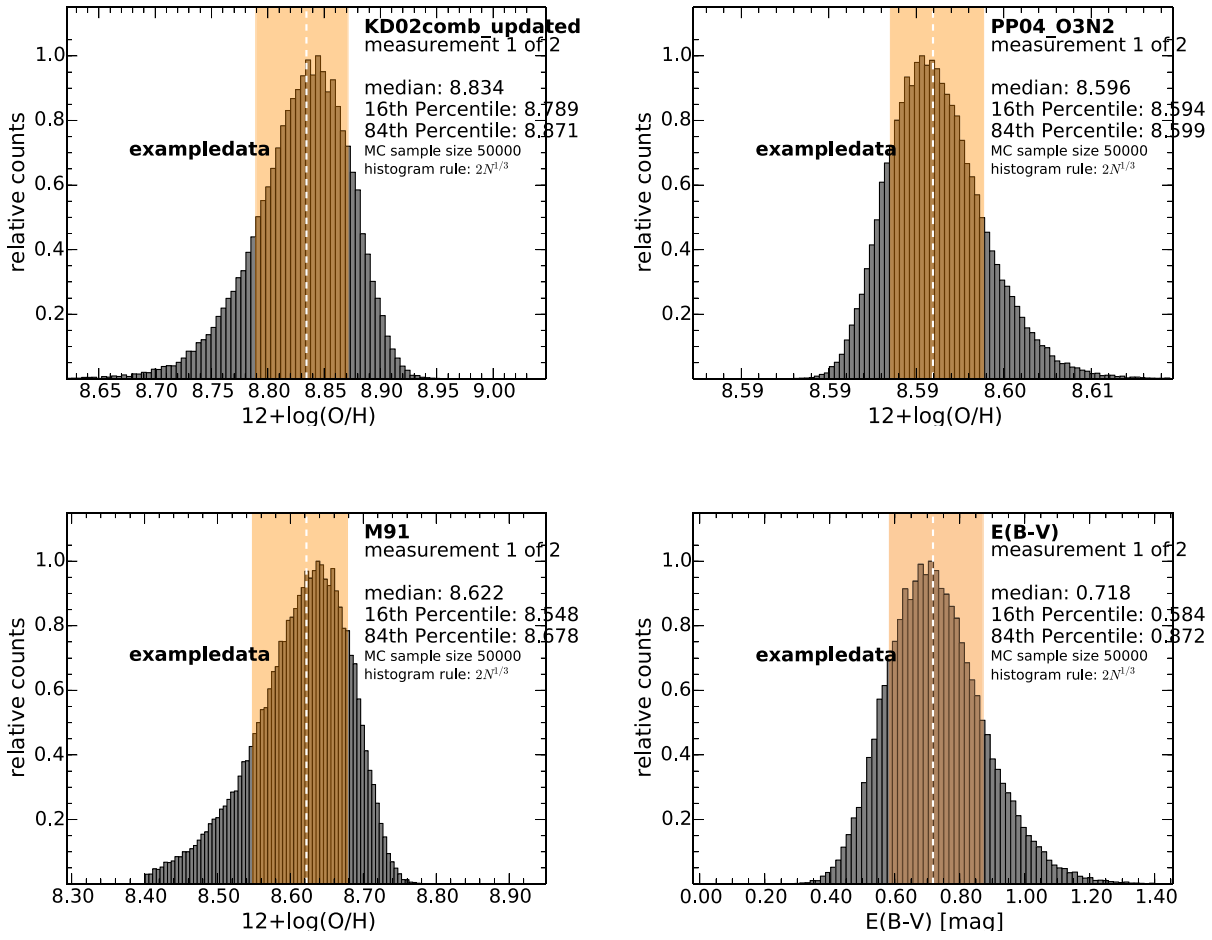

FIG. 1.— WILL UPDATE WITH NEW FIGURES BASED ON A PUBLISHED SN WITH SIGNFICANT E(B-V) AND WRITE MORE TEXT. Examples of confidence region determined by the algorithm, shaded in tan color.

other extinction laws and R_V values, if desired, given the code's open-source nature.

While other parameters, such as the ionization parameter q and the electron density (using the $SiII$ lines) are computed as long as the necessary lines are provided, they are not outputted in the current version of our code − however, the reader is welcome to easily modify the code to suite their needs, given it's an open-source code.

As output, we obtain metallicity values and their uncertainties in the following calibrations, as discussed in detail in Kewley & Dopita (2002); Kewley & Ellison (2008): Kewley & Dopita (2002)(KD02, for the 4 following computations: R23, using the NIIOII ratio, using the NII/Halpha ratio, and a combined method that uses the optimal method given the input line fluxes), McGaugh (1991) (M91), Zaritsky et al. (1994) (Z94), Pilyugin (2001) (P01), Denicoló et al. (2002) (D02), Pettini & Pagel (2004) (2 computations: PP04-N2, PP04-O3N2) **CHECK WITH FINAL CODE**. If the line fluxes necessary for specific scales are not provided, the output metallicities will -1 **CHECK WITH FINAL CODE**.

2.2. *Computing Uncertainties*

The novel aspect of our work is that we introduce a Monte Carlo (MC) resampling method to obtain numerous iterations via random sampling to obtain a more robust result for error estimation (e.g., Efron 1979; Hastie et al. 2009; Andrae 2010. Given a data set with error bars from which certain parameters are estimated, Monte Carlo resampling consists of resampling the data from its error distribution to produce alternative data sets. Here we generate a distribution of possible inputs by generating a gaussian error distribution centered on the measured line flux value, with a standard deviation corresponding to the measurement error, where we have made the assumption that the line flux error is gaussian distributed in nature[7]. Every iteration randomly takes an input value from this distribution (for each inputted line) to run the calculations. This effectively simulates conducting multiple experiments when repeated observation is impractical or impossible, as in the case of the emission line flux data, and thus generates alternative data sets. We generated N Monte Carlo samples of emission line fluxes (where an appropriate value of $N = 50,000$ is determined below) and calculated the metallicity for each set of line fluxes. At the end of N iterations, a parameter estimate distribution of oxygen abundance is generated for each scale by binning the results to histograms, and metallicity confidence regions are measured (see below)[8] . This is done for each scale. The fiftieth (50%) percentile, i.e. the median, is reported as the measured value. The output of our code includes the oxygen abundance measurements plus confidence regions in all scales, as well as plots of the likelihood distributions of the oxygen abundance value in all scales. Figure 1 shows the metallicity estimate distribution for 4 representative scales - those are the same plots that are outputted as part of our code for all scales (not all shown here). As can be seen, the metallicity distributions are rarely Gaussian, for two reasons: first, since the metallicities are computed based on log values of line flux ratios, symmetric error bars in linear space will translate into asymmetric error bars in log space; and seconds, since some metallicity computations (especially those that include R_{23}) are non-linear since they choose an upper vs lower branch by breaking the degeneracy.

This MC resampling approach takes into account the impact of the uncertain reddening (due to the uncertainties in the measurement of the Hα and Hβ fluxes), when the option for de-reddened metallicities is chosen. Since for each iteration, a new reddening value is calculated based on the resampled Hα and Hβ fluxes, which is used to compute the de-reddened metallicity value, the derived distribution of metallicity values takes into account the uncertain redding. As part of the optional output, a probability distribution plot for E(B-V) is provided (see last plot in figure 1, along with confidence intervals derived using the same method as for the metallicity measurements. If either Hα or Hβ flux is not provided, then no reddening correction can be applied and the computed metallicity will not be reddening-corrected and the E(B-V) output will be set to blank.

We note that our code does not output the *systematic* uncertainty of each scale, which are e.g., $\sim$ 0.07 dex (or 0.14 dex **CHECK**) for PP04-O2N2. Thus systematic errors can be as large, if not larger, than the statistical errors, however, if all metallicity measurements are in the *same* scale and only *relative* comparisons are made, then the systematic error does not have any impact (by definition!).

2.2.1. *Histogram Bin Size and Confidence Region*

Choosing the binning for a histogram is not trivial and Hogg (2008) describes various data analysis recipes for selecting a histogram bin size. Too many bins will result in many empty bins and an "over-fit" histogram, while too few bins may lose features of a probability distribution. While for our default option, we use Rice Rule (e.g., Hastie et al. 2009), namely using $2 * \sqrt[3]{N}$ as a number for our bins (which was appropriate for most of our test cases), we enable a number of binning options from which the user can choose, including Bayesian blocks, Knuth's rule and Doane's formula (**Fed's input here!**).

Since the metallicity distributions are rarely Gaussian, we cannot just fit a Gaussian and report the 1-σ intervals. In determining the confidence region intervals for asymmetric and multi-modal distributions, there are broadly three approaches (e.g., Andrae 2010): choosing a symmetric interval, the shortest interval , or a central interval. We determined the confidence interval using the "central" method, because it ensures that the algorithm finds the proper boundaries even in the case of multiple peaks (i.e., multimodal likelihood distributions) and for asymmetric, non-Gaussian, distributions. With the "central" method we determined the confidence interval by choosing the left and right boundaries such that the region outside the confidence interval each equally contains 16% of the total distribution for one standard deviation confidence interval - in analogy to the one-sigma-interval of the Gaussian distribution. While the

[7] In case the user provides their own probability distribution for the emission line uncertainties (e.g. from fitting Gaussians to the emission lines via MCMC methods, the user is welcome to easily modify the code to suite their needs, given its open-source nature

[8] However, note this method is a conservative approach, since it overestimates the intrinsic metallicity uncertainty, as we are centering this error distribution on the measured values instead of the (unknown) true values (Andrae 2010).

histograms at sufficiently high N, where N is the total number of iterations, yielded single peaked results, at lower N there were occasional multiple peaks resulting from a non-smooth gaussian being sampled. In selecting the value of N, we found that around $N = 50,000$ provides reliably smooth histograms.

In summary, the output for the measured value corresponds to the fiftieth (50%) percentile, while the lower error bar corresponds to the 50^{th}-16^{th} percentile and the upper error bar corresponds to 84^{th}-50^{th} of the metallicity parameter estimate distribution. However, we urge that the reader always inspect the appropriate metallicity distribution plots, which are also outputted, to check for themselves whether the outputted median and confidence regions properly represent the full metallicity distribution.

3. COMPARISON TO PRIOR UNCERTAINTY COMPUTATION AND OTHER WORKS

A previous method for determining the uncertainty in the oxygen abundance (as used in Modjaz et al. 2008; Kewley et al. 2010; Rupke et al. 2010; Modjaz et al. 2011) was an *analytic* approach of propagating the emission-line flux uncertainties: it found the maximum and minimum abundances via maximizing and minimizing, respectively, the various line ratios by adding/subtracting to the measured line values their uncertainties. For comparison we computed the metallicities and their errors in both ways (both analytic and using our current MC resampling method) for 3 representative scales. We plot our results and the residuals in Fig.2, which shows a number of important points: i) The metallicity reported as the 50th percentile of the metallicity parameter distribution from the MC resampling method is completely consistent with the analytically derived metallicity - well within the respective error bars - and thus, the prior published results still stand. ii) The MC resampling method has smaller error bars than the analytic method, especially for the scales of M91 and KD02. This is easily understandable, since the analytic method assumes the worst-case-scenario, as it basically yields 2 metallicity parameter draws (the "minimum" and "maximum") which are in the tail of the full metallicity probability/likelihood distribution. However, the MC resampling method is the more appropriate method as it empirically characterizes the full parameter estimation distribution.

3.1. *Comparison with other works*

The field SN host metallicity studies has been rapidly developing as these kinds of studies may be crucial avenues for constraining the progenitor systems of different kinds of explosions- however, many of the works do not show how they compute their statistical errors (e.g., Anderson et al. (2010); Leloudas et al. (2011); Sanders et al. (2012); Leloudas et al. (2014)). While Sanders et al. (2012) compute the line flux errors from a Markov-Chain Monte Carlo fitting of a gaussian to the emission lines, they only mention in passing that they propagate the line flux uncertainties into the metallicity measurements, but do not describe how.

In contrast, the general metallicity field has considered in detail how to estimate the uncertainties in measured metallicities- however, none of those codes are open-source and many of them are for specific scales which

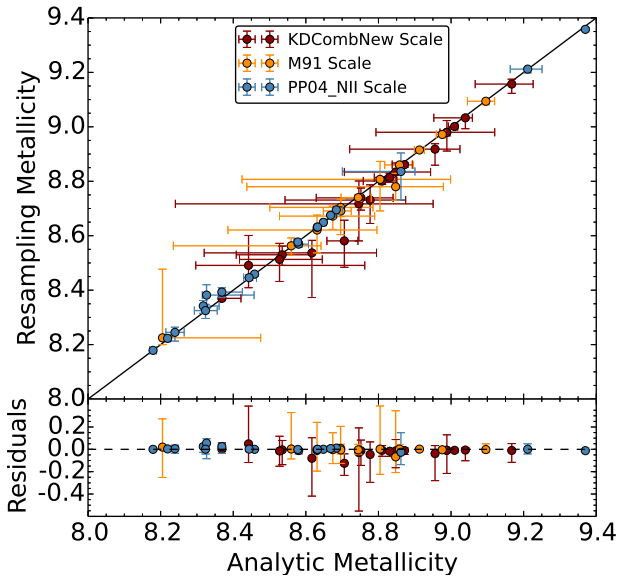

FIG. 2.— **FINISH**.Comparison of metallicity estimation between the analytic method and our Monte Carlo resampling method (top) and their residuals (bottom) for 3 different metallicity scales. Flux measurements come from 19 galaxies previously measured in Modjaz et al. (2011). To add asymmetric errors in quadrature we use $residual_{min} = \sqrt{x_{max}^2 + y_{min}^2}$ and $residual_{max} = \sqrt{x_{min}^2 + y_{max}^2}$.

were chosen by the authors: Moustakas et al. (2010) also use MC resampling to estimate the metallicity uncertainties (in their case using 500 trials which seems to lead to a Gaussian distribution) but only do this for two scale, KK04 and Pilyugin & Thuan (2005). For computing the metallicities of the SDSS star forming galaxies, Tremonti et al. (2004) fit a combination of stellar population synthesis and CLOUDY photoionization models to the observed strong emission lines [OII], Hbeta, OIII, Halpha, NII and SII and report the median of the metallicity likelihood distribution as the metallicity estimate, with the width of the distribution giving the 1 σ (Gaussian) error. However, this is constitutes their own scale, the T04 scale.

In the last stages of preparing this manuscript Blanc et al. (2015) was published. Blanc et al. (2015) employ Bayesian inference for doing something similar to Tremonti et al. (2004) - they use Bayesian inference to derive the joint and marginalized posterior probability density functions for metallicity and ionization parameter q given a set of observed line fluxes and an input photoionization model. They provide a publicly available IDL implementation of their method named IZI (inferring metallicities (Z) and ionization parameters) on the author's website.

4. CONCLUSIONS

FINISH. We hope that this open-access code will be used in many different fields where gas-phase metallicities are important, including in the emerging field of SN and GRB host galaxies, where either it is not described how they got or no error bars are computed (e.g., Lunnan et al. 2014).

M. Modjaz is supported in parts by the NSF CAREER

award AST-1352405 and by NSF award AST-1413260. This research made use of NASAs Astrophysics Data System; the NASA/IPAC Extragalactic Database (NED), which is operated by the Jet Propulsion Laboratory, California Institute of Technology, under contract with the National Aeronautics and Space Administration.

REFERENCES

Anderson, J. P., Covarrubias, R. A., James, P. A., Hamuy, M., & Habergham, S. M. 2010, MNRAS, 407, 2660
Andrae, R. 2010, ArXiv e-prints, arXiv:1009.2755
Asplund, M., Grevesse, N., Sauval, A. J., & Scott, P. 2009, ARA&A, 47, 481
Baldwin, J. A., Phillips, M. M., & Terlevich, R. 1981, PASP, 93, 5
Blanc, G. A., Kewley, L., Vogt, F. P. A., & Dopita, M. A. 2015, ApJ, 798, 99
Caffau, E., Ludwig, H.-G., Steffen, M., Freytag, B., & Bonifacio, P. 2011, Sol. Phys., 268, 255
Cardelli, J. A., Clayton, G. C., & Mathis, J. S. 1989, ApJ, 345, 245
Denicoló, G., Terlevich, R., & Terlevich, E. 2002, MNRAS, 330, 69
Dopita, M. A., Sutherland, R. S., Nicholls, D. C., Kewley, L. J., & Vogt, F. P. A. 2013, ApJS, 208, 10
Efron, R. 1979, Ann. Stat., 7, 1
Grevesse, N., Asplund, M., Sauval, A. J., & Scott, P. 2010, Ap&SS, 328, 179
Hastie, T., Tibshirani, R., & Friedman, J. 2009, The Elements of Statistical Learning: Data Mining, Inference, and Prediction (Springer Science+Business Media, New York)
Hogg, D. W. 2008, ArXiv e-prints, arXiv:0807.4820
Johnson, J. L., & Li, H. 2012, ApJ, 751, 81
Kauffmann, G., Heckman, T. M., Tremonti, C., et al. 2003, MNRAS, 346, 1055
Kelly, P. L., & Kirshner, R. P. 2012, ApJ, 759, 107
Kewley, L. J., & Dopita, M. A. 2002, ApJS, 142, 35
Kewley, L. J., & Ellison, S. L. 2008, ApJ, 681, 1183
Kewley, L. J., Groves, B., Kauffmann, G., & Heckman, T. 2006, MNRAS, 372, 961
Kewley, L. J., Rupke, D., Zahid, H. J., Geller, M. J., & Barton, E. J. 2010, ApJ, 721, L48
Kobulnicky, H. A., & Kewley, L. J. 2004, ApJ, 617, 240
Leloudas, G., Gallazzi, A., Sollerman, J., et al. 2011, A&A, 530, A95
Leloudas, G., Schulze, S., Kruehler, T., et al. 2014, ArXiv e-prints, arXiv:1409.8331
Levesque, E. M., Berger, E., Kewley, L. J., & Bagley, M. M. 2010, AJ, 139, 694
Lunnan, R., Chornock, R., Berger, E., et al. 2014, ApJ, 787, 138
Marino, R. A., Rosales-Ortega, F. F., Sánchez, S. F., et al. 2013, A&A, 559, A114
McGaugh, S. S. 1991, ApJ, 380, 140
Modjaz, M. 2012, in IAU Symposium, Vol. 279, IAU Symposium, 207–211
Modjaz, M., Kewley, L., Bloom, J. S., et al. 2011, ApJ, 731, L4
Modjaz, M., Kewley, L., Kirshner, R. P., et al. 2008, AJ, 135, 1136
Moustakas, J., Kennicutt, Jr., R. C., Tremonti, C. A., et al. 2010, ApJS, 190, 233
Osterbrock, D. E. 1989, Astrophysics of Gaseous Nebulae and Active Galaxies (Mill Vallery: University Science Books)
Pagel, B. E. J., Edmunds, M. G., Blackwell, D. E., Chun, M. S., & Smith, G. 1979, MNRAS, 189, 95
Pettini, M., & Pagel, B. E. J. 2004, MNRAS, 348, L59
Pilyugin, L. S. 2001, A&A, 369, 594
Pilyugin, L. S., & Thuan, T. X. 2005, ApJ, 631, 231
Rupke, D. S. N., Kewley, L. J., & Chien, L.-H. 2010, ApJ, 723, 1255
Sanders, N. E., Soderberg, A. M., Levesque, E. M., et al. 2012, ApJ, 758, 132
Simón-Díaz, S., & Stasińska, G. 2011, A&A, 526, A48+
Stasińska, G. 2002, ArXiv Astrophysics e-prints, astro-ph/0207500
Tremonti, C. A., Heckman, T. M., Kauffmann, G., et al. 2004, ApJ, 613, 898
Zaritsky, D., Kennicutt, Jr., R. C., & Huchra, J. P. 1994, ApJ, 420, 87

APPENDIX

MINIMUM CODE VALIDATION

WORK WITH FED - and any other code specific things